Title

Coronin Enhances Actin Filament Severing by Recruiting Cofilin to Filament Sides and Altering F-Actin Conformation

Journal

Journal of Molecular Biology, 427(19)

ISSN

0022-2836

Authors

Mikati, Mouna A
Breitsprecher, Dennis
Jansen, Silvia
et al.

Publication Date

2015-09-01

DOI

10.1016/j.jmb.2015.08.011

HHS Public Access

Author manuscript

J Mol Biol. Author manuscript; available in PMC 2016 September 25.

Published in final edited form as:

J Mol Biol. 2015 September 25; 427(19): 3137–3147. doi:10.1016/j.jmb.2015.08.011.

Coronin enhances actin filament severing by recruiting cofilin to filament sides and altering F-actin conformation

Mouna A. Mikati[1,*], **Dennis Breitsprecher**[2,*], **Silvia Jansen**[2], **Emil Reisler**[1,#], and **Bruce L. Goode**[2,#]

[1]Department of Chemistry and Biochemistry and Molecular Biology Institute, University of California, Los Angeles, CA, 90095, USA

[2]Department of Biology, Rosenstiel Basic Medical Science Research Center, Brandeis University, Waltham, MA, 02454, USA

Abstract

High rates of actin filament turnover are essential for many biological processes, and require the activities of multiple actin-binding proteins working in concert. The mechanistic role of the actin filament severing protein cofilin is now firmly established; however, the contributions of other conserved disassembly-promoting factors including coronin have remained more obscure. Here, we have investigated the mechanism by which yeast coronin (Crn1) enhances F-actin turnover. Using multi-color total internal reflection (TIRF) microscopy, we show that Crn1 enhances Cof1-mediated severing by accelerating Cof1 binding to actin filament sides. Further, using biochemical assays to interrogate F-actin conformation, we show that Crn1 alters longitudinal and lateral actin-actin contacts and restricts opening of the nucleotide-binding cleft in actin subunits. Moreover, Crn1 and Cof1 show opposite structural effects on F-actin, yet synergize in promoting release of phalloidin from filaments, suggesting that Crn1/Cof1 co-decoration may increase local discontinuities in filament topology to enhance severing.

Graphical Abstract

[#]Authors for correspondence: Dr. Bruce L. Goode, Tel: (781) 736-2464, Fax: (781) 736-2405, goode@brandeis.edu. Dr. Emil Reisler, Tel: (310) 825-2668, Fax: (310) 206-4038, reisler@mbi.ucla.edu.

[*]These authors contributed equally to this work

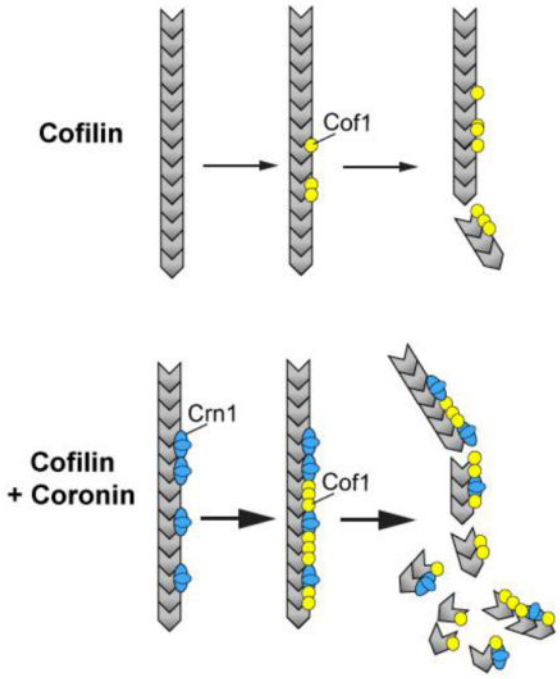

Keywords

actin; severing; cofilin; coronin; cross-linking

Introduction

Multiple actin-associated proteins working in concert are required to maintain the high rates of actin filament disassembly and turnover that drive processes such as cell motility, cell division, and endocytosis [1, 2]. Among the most conserved and ubiquitously expressed F-actin disassembly factors are ADF/cofilin, coronin, Aip1, and Srv2/CAP, of which only the mechanism of ADF/cofilin has been well defined[3, 4]. The remaining proteins are likely to each make unique contributions to promoting actin filament turnover, but their mechanisms are currently not well understood [5–7].

ADF/cofilin (herein referred to as cofilin) is essential in vivo for actin-based processes that require high rates of actin turnover, including endocytosis, cell motility, and cytokinesis [8–11]. In vitro studies using total internal reflection fluorescence (TIRF) microscopy, cryo-electron microscopy, and atomic force microscopy have shown that cofilin binds preferentially and cooperatively to the sides of older (ADP-bound) regions of actin filaments, promotes cation release, alters the twist of filaments, and changes the lateral and longitudinal actin-actin contacts in filaments [12–16]. These structural effects propagate from the site of cofilin binding toward the pointed end of the filament [17], and lead to severing events at boundaries between cofilin-decorated (destabilized) and bare (stabilized) patches [17, 18].

Despite the remarkable structural and mechanistic detail in which the actions of cofilin have been described, there remain several unsolved puzzles. For instance, direct observation of cofilin severing of filaments by single and multi-wavelength TIRF microscopy [18–20] has shown that cofilin binding to F-actin is quite slow (1.3×10^4 s^{-1} M^{-1}), and that severing by cofilin alone is relatively inefficient (0.002 severing events per μm F-actin per sec). However, the above-mentioned disassembly co-factors (coronin, Aip1, and Srv2/CAP) are believed to work in concert with cofilin to improve the efficiency of severing. Indeed, recent studies have begun to focus on understanding how cofilin functions together with Aip1, Srv2/CAP, and coronin to acheive enhanced actin disassembly [21–28]. Here, we focus on the role and mechanism of coronin in increasing the efficiency of cofilin-mediated actin filament severing.

Coronin is a 50–70 kDa conserved F-actin binding protein that was first identified in *Dictyostelium*, where it plays an important role in actin-based processes such as cell motility, phagocytosis, and endocytosis [29–31]. Since then, coronins have been identified in a wide range of organisms, including yeast and mammals, and linked to a multitude of actin-based cellular and physiological processes [6, 32]. One of the earliest clues about how coronins might contribute mechanistically to regulating actin dynamics was the observation that mutations in the budding yeast homolog of coronin (Crn1) are synthetic lethal with partial loss-of-function mutations in *cof1* [33]. Subsequently, in vivo studies in both yeast and mammalian cells demonstrated directly that coronins promote the rapid turnover of cellular actin structures [34, 35]. On the other hand, the mechanism underlying these effects has remained only partially defined. In vitro, purified coronins were found to bind preferentially to ATP/ADP+Pi− compared to ADP-F-actin, and to inhibit F-actin disassembly by cofilin [34, 35]. Further, these inhibitory effects of yeast Crn1 were shown to be nucleotide state-specific, with Crn1 blocking Cof1-mediated severing of ATP/ADP+Pi−F-actin but enhancing severing of ADP-F-actin [35]. Together, these results have suggested that coronin may exclude cofilin from binding ATP-F-actin. In line with that a recent EM study demonstrated that Crn1 interactions with F-actin are distinct for ADP−P_i versus ADP-F-actin, and only when Crn1 is bound to ADP-F-actin is there room for adjacent binding of cofilin [36]. Thus, coronin appears to somehow ‘prime’ ADP-F-actin for cofilin binding and subsequent severing.

More recently, we provided new insights into the coronin mechanism in real time using in vitro multi-wavelength TIRF microscopy, showing that mouse Coronin-1B binds rapidly to F-actin and accelerates recruitment of human Cofilin-1 to filament sides to enhance severing [24]. In the present study, we have addressed the lingering question of whether this mechanism extends to coronin in other species, focusing on yeast Crn1 and Cof1, and investigated the structural basis for coronin’s effects in enhancing actin filament severing.

Results

Crn1ΔCC strongly enhances Cof1-mediated severing of actin filaments

In a previous study, we showed using bulk kinetic assays that yeast coronin (Crn1ΔCC, 1–600; which lacks the C-terminal coiled coil domain) enhances Cof1-mediated actin disassembly[35]. Here, to gain mechanistic insights into these effects, we used TIRF

microscopy to directly visualize the effects of Crn1ΔCC on Cof1-mediated severing of filaments in real time. In these assays, fluorescently labeled filaments (10% Oregon Green-labeled actin; 0.5% biotin-labeled actin) were polymerized and tethered to the coverslip. Once filaments grew to a length of 10–15 μm, actin monomers were washed out, then cofilin and/or coronin were introduced and severing was monitored for 150 s (Fig. 1). Importantly, in these assays the preassembled filaments are primarily in an ADP-state by the point they are exposed to cofilin and/or coronin. Severing was observed specifically in the presence of Cof1, and quantification of the data showed that Crn1ΔCC enhanced severing by approximately 6-fold (Fig. 1).

Crn1ΔCC accelerates recruitment of Cy3-Cof1 to actin filament sides

To better define the underlying mechanism by which Crn1ΔCC enhances Cof1-mediated severing, we performed two-color TIRF experiments using Cy3-labeled Cof1 [20], which allowed us to directly monitor Cof1 binding to filaments leading to severing events. As previously demonstrated, Cy3-Cof1 alone exhibited cooperative binding to filaments, and induced fragmentation at sites between Cof1-decorated and undecorated regions [18, 20]. Addition of Crn1ΔCC led to a dramatic increase in the rate of Cy3-Cof1 accumulation on filament sides (Fig. 2A and B). Interestingly, there was no significant difference in the intensity of Cy3-Cof1 fluorescence spots where severing occured (Fig. 2C and D), suggesting that enhanced severing by Crn1ΔCC stems from an increase in the number of Cof1 spots that accumulate on filaments rather than an increase in Cof1 spot density at severing sites. In addition, our analysis revealed that the presence of Crn1ΔCC does not alter substantially the time interval between appearance of a Cy3-Cof1 spot on a filament and subsequent severing (Fig. 2E and F). This again suggests that Crn1ΔCC enhances severing primarily by increasing the kinetics of Cof1 recruitment to filament sides.

Crn1ΔCC interactions alter the dynamic states of longitudinal and lateral subunit contact elements in F-actin

To probe the structural basis for Crn1ΔCC increasing Cof1 recruitment to actin filament sides, we asked whether Crn1ΔCC alters the subunit contacts in F-actin, as detected by cysteine cross-linking. We first monitored the stability of longitudinal actin-actin contacts in filaments using a Q41C actin mutant [12]. This mutated residue is located in the D-loop of actin, and upon polymerization it comes into close proximity with C374 on the adjacent actin protomer and readily forms a disulfide bridge with that residue (Fig. 3A). Cross-linking of polymerized Q41C actin was induced in the presence and absence of Crn1ΔCC and monitored over time via SDS-PAGE, quantifying the rate of disappearance of the uncross-linked actin monomer band. In the presence of Crn1ΔCC, cross-linking of C41 to C374 was greatly accelerated (Fig. 3B and C) and the initial rate constant of cross-linking was about 5-fold faster than in the absence of Crn1ΔCC. These results suggest that Crn1ΔCC decoration of F-actin decreases the time average distance between C41 and C374, and/or limits the fluctuations of D-loop elements to positions favoring the 41–374 cross-linking, and thereby stabilizes longitudinal contacts in F-actin.

A similar approach was used to analyze changes in the lateral actin-actin contacts in filaments. For these experiments, we used a different mutant actin, S265C, in which the

mutated residue resides within the hydrophobic loop (H-loop) and can thus interact with C374 of a neighboring subunit (Fig. 3D). After induction of cross-linking, the temporal pattern on gels was again strikingly different in the presence of Crn1ΔCC. However, in this case Crn1ΔCC inhibited the initial cross-linking rate by 6-fold (Fig. 3E and F). These results suggest that Crn1ΔCC binding to F-actin causes an increase in the mean distance between the hydrophobic loop and C374, and thus modifies native lateral subunit contacts in F-actin.

Crn1ΔCC locks the nucleotide binding cleft on actin into a more open position

We next probed the effects of Crn1ΔCC on the nucleotide binding cleft of actin using a double mutant Q59C/D211C. Residues 59 and 211 are located on either side of the nucleotide-binding cleft of actin, in subdomains 2 and 4 (SD2 and SD4), respectively (Fig. 4A). Cross-linking of this mutant was performed using homo-bi-functional thiol-specific reagents called methanothiosulfonates (MTS), which have different average spacer arm lengths and can be used as molecular rulers. Our results show that Crn1ΔCC decreases the rate of cross-linking specifically when MTS1 (5.4Å) is used, but has the opposite effect when MTS2 (5.9Å) is used, and has no effect when MTS3 (6.4Å) is used (Fig. 4B and C). Together, these observations suggest that Crn1ΔCC alters the nucleotide binding cleft of actin such that it is less flexible, stabilizing it in a more open conformation.

Crn1ΔCC and Cof1 have opposite effects on F-actin structure and dynamics

The increase in cross-linking rate of C41 to C374 implies that Crn1ΔCC stabilizes D-loop states that promote this cross-linking pattern, and stabilizes longitudinal actin-actin interactions. This is in sharp contrast to the effect of cofilin on 41–374 cross-linking and the overall D-loop dynamics in F-actin [12, 14, 37]. To gain confidence in this conclusion, we expanded the probing of D-loop dynamics via additional cross-linking reactions. Specifically, we compared the effects of Crn1ΔCC and Cof1 on the cross-linking of F-actin co-polymerized from an equal mixture of two mutants, K50C/C374A and S265C/C374A (we refer to the mixture as C50/C265). This crosslinking strategy generates a lateral bond between cysteines in the D-loop and the H-loop (Fig. 5A), blocking polymerization and leading to the formation of amorphous actin aggregates [38]. This analysis revealed that Cof1 increases the rate of cross-linking, whereas Crn1ΔCC decreases it strongly (Fig. 5B and C). As 50–265 cross-linking can be ascribed to dynamic fluctuations of D-loop, which can transiently bring C50 close to C265, Crn1ΔCC and cofilin have clearly opposite effects on D-loop dynamics. It is possible that the relative stabilization of D-loop's conformation in the presence of Crn1ΔCC is assisted by ionic interactions of actin's R37, R39 and K50 on its D-loop with coronin's E320 and D250, D273, respectively, as identified in the proposed model of Crn1ΔCC-ADP-F-actin structure [36].

Despite these differences Crn1ΔCC and Cof1 each rescued the polymerization of C50/C265 cross-linked actin, enabling it to form filaments rather than aggregates, as indicated by an increase in light scattering (Fig. 5D) and verified by EM (Fig. 5E). The simplest explanation for such rescue is that both proteins bind two actin protomers, and can therefore substitute for some of the stabilizing actin-actin contacts lost in the mutant and modified actins.

Crn1ΔCC and Cof1 synergistically induce the release of phalloidin from filaments

Interestingly, the polymerization rescue by Crn1ΔCC and Cof1 described above can be achieved also with phalloidin [38]. Rhodamine phalloidin binds to three actin subunits across filament strands, stabilizing mainly lateral (but also longitudinal) contacts in F-actin and reducing the critical concentration for polymerization by two orders of magnitude [39]. This helps to explain why phalloidin rescues the polymerization of the oxidized C50/C265 mutant [38]. Prompted by the observations that cofilin and phalloidin compete for the binding to F-actin, and that cofilin induces slow release of rhodamine phalloidin from F-actin (Fig 6) [13], we also investigated whether Crn1ΔCC, alone or together with Cof1, competes with phalloidin for binding F-actin. This was accomplished in competition assays that report on rhodamine phalloidin release from F-actin via loss of fluorescence. Our analysis showed that Crn1ΔCC alone has no appreciable effect on the rate of phalloidin release, suggesting that it does not induce major conformational changes in the lateral interface of the filament that would interfere with binding of phalloidin (Fig. 6). On the other hand, in the presence of Cof1, Crn1ΔCC strongly increased the rate of phalloidin release from F-actin (Fig. 6), consistent with the observed ability of Crn1ΔCC to enhance recruitment of Cof1 to filaments and/or synergistic structural effects derived from co-decoration of filaments by Crn1ΔCC and Cof1.

DISCUSSION

In this study we have investigated the mechanistic basis for yeast Crn1 regulating Cof1-mediated actin filament disassembly. By directly visualizing the mechanism in real time, we observed that Crn1 dramatically accelerates recruitment of Cy3-Cof1 to the sides of filaments (comprised primarily of ADP-actin) and increases the rate of severing by 6-fold. However, Crn1 did not alter substantially the distribution of Cy3-Cof1 spot intensities on filaments prior to severing events, nor the time interval from first appearance of Cy3-Cof1 to severing. Thus, Crn1 appears to enhance severing primarily by accelerating Cof1 binding to ADP-actin filaments. These effects for yeast Crn1 and Cof1 are similar to our recent observations for mouse Coronin-1B and human Cofilin-1 [24], and thus the mechanism by which coronin influences cofilin-mediated actin filament severing appears to be highly conserved across evolutionarily distant species.

The mechanism we have defined for coronin is particularly fascinating because it is precisely opposite and complementary to that of Srv2/CAP. Unlike coronin, Srv2/CAP does not improve the binding of cofilin to filaments, but instead binds to filaments (independently of cofilin) and reduces the time interval from cofilin binding to severing [20, 25]. Thus, coronin and Srv2/CAP have distinct roles in increasing the efficiency of severing by cofilin. Further, recent evidence suggests that Aip1 makes yet another distinct contribution to filament severing and disassembly [23, 24]. Not surprisingly therefore, loss of different pairs of these co-factors in vivo leads to severely compromised cell growth or lethality, e.g., *srv2*Δ*aip1*Δ and *crn1*Δ*srv2*Δ ([40] and B.G., unpublished data). These observations also highlight the importance of the co-factor-driven mechanisms in maintaining high rates of actin turnover required for normal cellular functions.

How then does coronin recruit cofilin to F-actin to enhance filament severing? One possible model is that coronin alters the conformation of F-actin to favor cofilin binding. Earlier EM studies on the decoration of ATP/ADP+P_i−F-actin by coronin suggested that coronin and cofilin binding sites on F-actin are partially overlapping and thus would lead to steric clashes, preventing co-decoration in close proximity [14]. However, a more recent study found that the position of coronin shifts on ADP-F-actin compared to ATP/ADP+P_i−F-actin, such that co-decoration is possible [36]. Therefore, coronin may increase cofilin binding by providing it with additional or alternate contact sites on the coronin-actin complex. Using cysteine crosslinking analysis we found that coronin alters F-actin structure in several ways. First, coronin altered the nucleotide binding cleft of actin, keeping it in a more open position and preventing it from attaining its most closed conformation. In yeast actin, P_i release is concurrent with polymerization, and it has been suggested there is a delayed conformational change in F-actin after P_i release, which yields “mature” filaments [41, 42]. In another study [43], it was shown that such maturation of skeletal muscle ADP-F-actin led to enhanced and/or accelerated severing of filaments by cofilin. Thus, coronin could possibly recruit cofilin by catalyzing this conformational conversion (maturation) following P_i release. Second, our data showed that coronin binding destabilizes lateral contacts between actin subunits in the filament, similar to the effects of cofilin [13]. However, all other tests indicated opposite effects of coronin and cofilin on filament structural dynamics, especially that of the D-loop on actin, and their overall stability. These results are consistent with the above mentioned possibility that coronin itself provides additional contacts for cofilin to improve cofilin’s affinity for F-actin, and to help attract cofilin to sites where coronin is already bound.

Finally, our data suggest that coronin may enhance cofilin-mediated severing not only by accelerating cofilin recruitment to filament sides, but also by working in concert with cofilin to alter filament conformation and stability. As mentioned above, coronin and cofilin each destabilize lateral actin-actin contacts in adjacent protomers of F-actin. Specifically, they reduce insertion of the H-loop on one actin subunit into the hydrophobic pocket of the adjacent subunit on the opposite strand of the filament. Since this interaction is required for F-actin stability [44], coronin and cofilin may work in concert to more rapidly destabilize filaments and thereby increase the rate of severing. Further, coronin and cofilin binding may produce distinct conformational effects on F-actin and thus increase discontinuities in filament topology to accelerate fragmentation. Indeed, such a possibility is indicated by the opposite effects of coronin and cofilin on C41-C374 and C50-C265 crosslinking, suggesting that they do have distinct structural effects on F-actin. In this manner, binding of coronin interspersed with cofilin on filaments may amplify the boundaries between cofilin-decorated and undecorated regions to increase severing efficiency [45].

MATERIALS AND METHODS

Protein expression and purification

GST-tagged Crn1ΔCC constructs were expressed in Rosetta 2 DE3 cells and purified from the soluble fractions first on Glutathione-Uniflow Resin (Clontech Laboratories), then on-column thrombin cleavage overnight at 4 °C, and gel filtration (Superdex 75). Skeletal actin was isolated from rabbit muscle [46]. Wild type and mutant yeast actins, Cof1, Crn1ΔCC, and

the Cof1 (T46C) mutant used for Cy3-labeling were purified as described [20, 35, 47]. Biotin- and OG-labeled skeletal actins used in TIRF assays were prepared as described [48].

Multi-wavelength total internal reflection fluorescence (TIRF) microscopy

Multi-wavelength TIRF microscopy was performed on pre-polymerized biotin-tethered OG-labeled actin filaments as described[20]. Briefly, acid-washed coverslips were coated with PEG-silane and PEG-biotin silane; and assembled into flow cells. Flow cells were incubated for 5 min with HBSA (HEK buffer with 1% BSA), followed by 30 s incubation with 0.1 mg/ml Streptavidin in PBS, then washed with 5 chamber volumes (~50 μl) HBSA, and equilibrated with 1X TIRF buffer (10 mM imidazole, 50 mM KCl, 1 mM $MgCl_2$, 1 mM EGTA, 0.2 mM ATP, 10 mM DTT, 15 mM glucose, 20 μg/ml catalase, 100 μg/ml glucose oxidase, and 0.5% methylcellulose (4000 cP), pH 7.5). Reactions were initiated by rapidly diluting actin monomers (final 1 μM, 10% OG-labeled, 0.5% biotinylated) into 1X TIRF buffer and transferring the mixture to a flow chamber. Filaments were polymerized until they reached lengths of approximately 10–15 μm, and then the reaction mixture was replaced with TIRF buffer containing Cof1 and/or Crn1ΔCC polypeptides, but lacking actin monomers. Time-lapse imaging of OG-actin filaments and Cy3-Cof1 were performed using a Nikon-Ti200 inverted microscope equipped with 150-mW Ar-Laser and 5-mW He-Ne lasers (Mellot Griot, Carlsbad, CA), a TIRF objective with a 1.49 numerical aperture (Nikon, New York, NY), and an EMCCD camera (Andor Ixon, Belfast, Northern Ireland). During measurements, optimal focus was maintained using the Perfect Focus System (Nikon). Images were captured every 3–5 s. The pixel size corresponded to 0.27 μm. Acquired image sequences were converted to 16-bit TIFF files with ImageJ (http://imagej.nih.gov/ij) using the NIS-to-ImageJ plug-in (Nikon). Background fluorescence for each channel was subtracted automatically using the background subtraction tool (rolling ball radius: 50 pixel) implemented in the ImageJ software. Filament-severing efficiency, expressed as severing events per μm of F-actin per sec, was determined by measuring the lengths of each filament using ImageJ prior to flow in, and then counting severing events over a 200 s window after addition of Cof1 and/or Crn1ΔCC. No severing events were observed for Crn1ΔCC in the absence of Cof1. Dual-color TIRF experiments using Cy3-Cof1 and OG-actin were carried out essentially as single-color experiments with the exception that OG and Cy3 fluorescence was detected sequentially, with excitation times of 50 and 300 ms, respectively. Fluorescence intensities of Cy3-Cof1 spots at severing sites were obtained by integrating the fluorescence intensity in a boxed region of 4 × 4 pixels at severing sites one frame prior to when severing occurred.

Cysteine cross-linking of subunits in actin filaments

Free thiols were removed from samples of yeast actin cysteine mutants using Sephadex G-50 spin columns equilibrated with G-buffer containing 10 mM Hepes pH 7.5, 0.2 mM $CaCl_2$ and 0.2 mM ATP. Actin was polymerized for 2 hr on ice by the addition of 3 mM $MgCl_2$ and 50mM KCl. Saturating amounts (1:1) of Crn1ΔCC and Cof1 to F-actin were added. Disulfide cross-linking of actin mutants was catalyzed by addition of 5 μM $CuSO_4$ or 10 μM MTS reagents, and samples of the reaction were removed and stopped by the addition of 2mM N-ethyl maleimide (NEM). The kinetics of disulfide cross-linking were

monitored by SDS-PAGE under non-reducing conditions. The decay of the actin monomer band that accompanied cross-linking was quantified using Scion Image software.

Light-scattering and rhodamine-phalloidin release assay

Rescue of actin polymerization and disulfide cross-linking were monitored by light-scattering in a PTI fluorometer at 325 nm for both excitation and emission wavelengths. Phalloidin was obtained from Sigma and rhodamine phalloidin was obtained from Molecular Probes (Eugene, OR). 100 nM yeast F-actin (in 10 mM Hepes, 3.0 mM $MgCl_2$, 50 mM KCl, 0.2 mM $CaCl_2$, 0.2 mM ATP, 1 mM DTT at pH 7.4) was pre-incubated overnight on ice with 0.2 μM rhodamine phalloidin and 4.8 μM phalloidin. Rhodamine phalloidin fluorescence was monitored using a PTI fluorometer at 575 nm emission before and after addition of Crn1ΔCC and/or Cof1 (5.5 μM each).

Electron microscopy (EM)

Undiluted samples from actin polymerization reactions (Fig. 5D) were applied to carbon-coated grids and stained with 1% uranyl acetate. Samples were handled with special care, using slow pipetting and cut tips to avoid filament shearing. This was important for the coronin-decorated filaments since EM imaging showed they were more susceptible to mechanical breakage (M.M. and E.R., unpublished observations). Similar effects were observed for metavinculin-decorated actin filaments, which have a decreased persistence length (3.9 ± 0.5 μm and 8.4 ± 0.2 μm for decorated and bare filaments, respectively [49]). We therefore speculate that coronin may also reduce the rigidity of actin filaments, making them more prone to bending. The grids were examined in a Hitachi H7000 electron microscope under minimal-dose conditions at an accelerating voltage of 75 keV and a nominal magnification of 40,000.

Supplementary Material

Refer to Web version on PubMed Central for supplementary material.

Acknowledgments

We are grateful to Dr. M. Gandhi and F. Chaudhry for providing some of the proteins used in TIRF experiments, and to Dr. M.L. Phillips (UCLA) for assistance with electron microscopy. We thank Dr. Durer (UCLA) for the EM image showing the products of polymerization of cross-linked C50/C265 actin in the presence of Cof1 (Figure 5E). This work was supported by grants from NIH to E.R. (GM077190) and B.G. (GM063691).

Abbreviations

MTS methanothiosulfonates

References

1. Bugyi B, Carlier MF. Control of actin filament treadmilling in cell motility. Annual review of biophysics. 2010; 39:449–470.
2. Pollard TD, Borisy GG. Cellular motility driven by assembly and disassembly of actin filaments. Cell. 2003; 112:453–465. [PubMed: 12600310]

3. Bamburg JR, McGough A, Ono S. Putting a new twist on actin: ADF/cofilins modulate actin dynamics. Trends in cell biology. 1999; 9:364–370. [PubMed: 10461190]
4. Hild G, Kalmar L, Kardos R, Nyitrai M, Bugyi B. The other side of the coin: functional and structural versatility of ADF/cofilins. European journal of cell biology. 2014; 93:238–251. [PubMed: 24836399]
5. Brieher W. Mechanisms of actin disassembly. Molecular biology of the cell. 2013; 24:2299–2302. [PubMed: 23900650]
6. Chan KT, Creed SJ, Bear JE. Unraveling the enigma: progress towards understanding the coronin family of actin regulators. Trends in cell biology. 2011; 21:481–488. [PubMed: 21632254]
7. Ono S. The role of cyclase-associated protein in regulating actin filament dynamics - more than a monomer-sequestration factor. Journal of cell science. 2013; 126:3249–3258. [PubMed: 23908377]
8. Bravo-Cordero JJ, Magalhaes MA, Eddy RJ, Hodgson L, Condeelis J. Functions of cofilin in cell locomotion and invasion. Nature reviews Molecular cell biology. 2013; 14:405–415. [PubMed: 23778968]
9. Chen Q, Pollard TD. Actin filament severing by cofilin is more important for assembly than constriction of the cytokinetic contractile ring. The Journal of cell biology. 2011; 195:485–498. [PubMed: 22024167]
10. Lappalainen P, Drubin DG. Cofilin promotes rapid actin filament turnover in vivo. Nature. 1997; 388:78–82. [PubMed: 9214506]
11. Mendes Pinto I, Rubinstein B, Kucharavy A, Unruh JR, Li R. Actin depolymerization drives actomyosin ring contraction during budding yeast cytokinesis. Developmental cell. 2012; 22:1247–1260. [PubMed: 22698284]
12. Bobkov AA, Muhlrad A, Kokabi K, Vorobiev S, Almo SC, Reisler E. Structural effects of cofilin on longitudinal contacts in F-actin. Journal of molecular biology. 2002; 323:739–750. [PubMed: 12419261]
13. Bobkov AA, Muhlrad A, Shvetsov A, Benchaar S, Scoville D, Almo SC, Reisler E. Cofilin (ADF) affects lateral contacts in F-actin. Journal of molecular biology. 2004; 337:93–104. [PubMed: 15001354]
14. Galkin VE, Orlova A, Kudryashov DS, Solodukhin A, Reisler E, Schroder GF, Egelman EH. Remodeling of actin filaments by ADF/cofilin proteins. Proceedings of the National Academy of Sciences of the United States of America. 2011; 108:20568–20572. [PubMed: 22158895]
15. Kang H, Bradley MJ, Cao W, Zhou K, Grintsevich EE, Michelot A, Sindelar CV, Hochstrasser M, De La Cruz EM. Site-specific cation release drives actin filament severing by vertebrate cofilin. Proceedings of the National Academy of Sciences of the United States of America. 2014; 111:17821–17826. [PubMed: 25468977]
16. McGough A, Pope B, Chiu W, Weeds A. Cofilin changes the twist of F-actin: implications for actin filament dynamics and cellular function. The Journal of cell biology. 1997; 138:771–781. [PubMed: 9265645]
17. Ngo KX, Kodera N, Katayama E, Ando T, Uyeda TQ. Cofilin-induced unidirectional cooperative conformational changes in actin filaments revealed by high–speed atomic force microscopy. eLife. 2015:4.
18. Suarez C, Roland J, Boujemaa-Paterski R, Kang H, McCullough BR, Reymann AC, Guerin C, Martiel JL, De la Cruz EM, Blanchoin L. Cofilin tunes the nucleotide state of actin filaments and severs at bare and decorated segment boundaries. Curr Biol. 2011; 21:862–868. [PubMed: 21530260]
19. Andrianantoandro E, Pollard TD. Mechanism of actin filament turnover by severing and nucleation at different concentrations of ADF/cofilin. Molecular cell. 2006; 24:13–23. [PubMed: 17018289]
20. Chaudhry F, Breitsprecher D, Little K, Sharov G, Sokolova O, Goode BL. Srv2/cyclase-associated protein forms hexameric shurikens that directly catalyze actin filament severing by cofilin. Molecular biology of the cell. 2013; 24:31–41. [PubMed: 23135996]
21. Brieher WM, Kueh HY, Ballif BA, Mitchison TJ. Rapid actin monomer-insensitive depolymerization of Listeria actin comet tails by cofilin, coronin, and Aip1. The Journal of cell biology. 2006; 175:315–324. [PubMed: 17060499]

22. Chen Q, Courtemanche N, Pollard TD. Aip1 promotes actin filament severing by cofilin and regulates the constriction of the cytokinetic contractile ring. The Journal of biological chemistry. 2014
23. Gressin L, Guillotin A, Guerin C, Blanchoin L, Michelot A. Architecture dependence of actin filament network disassembly. Curr Biol. 2015; 25:1437–1447. [PubMed: 25913406]
24. Jansen S, Collins A, Chin SM, Ydenberg CA, Gelles J, Goode BL. Single-molecule imaging of a three-component ordered actin disassembly mechanism. Nature communications. 2015; 6:7202.
25. Jansen S, Collins A, Golden L, Sokolova O, Goode BL. Structure and Mechanism of Mouse Cyclase-associated Protein (CAP1) in Regulating Actin Dynamics. The Journal of biological chemistry. 2014; 289:30732–30742. [PubMed: 25228691]
26. Nadkarni AV, Brieher WM. Aip1 destabilizes cofilin-saturated actin filaments by severing and accelerating monomer dissociation from ends. Curr Biol. 2014; 24:2749–2757. [PubMed: 25448002]
27. Normoyle KP, Brieher WM. Cyclase-associated protein (CAP) acts directly on F-actin to accelerate cofilin-mediated actin severing across the range of physiological pH. The Journal of biological chemistry. 2012; 287:35722–35732. [PubMed: 22904322]
28. Okada K, Blanchoin L, Abe H, Chen H, Pollard TD, Bamburg JR. Xenopus actin-interacting protein 1 (XAip1) enhances cofilin fragmentation of filaments by capping filament ends. The Journal of biological chemistry. 2002; 277:43011–43016. [PubMed: 12055192]
29. de Hostos EL, Bradtke B, Lottspeich F, Guggenheim R, Gerisch G. Coronin, an actin binding protein of Dictyostelium discoideum localized to cell surface projections, has sequence similarities to G protein beta subunits. The EMBO journal. 1991; 10:4097–4104. [PubMed: 1661669]
30. de Hostos EL, Rehfuess C, Bradtke B, Waddell DR, Albrecht R, Murphy J, Gerisch G. Dictyostelium mutants lacking the cytoskeletal protein coronin are defective in cytokinesis and cell motility. The Journal of cell biology. 1993; 120:163–173. [PubMed: 8380174]
31. Maniak M, Rauchenberger R, Albrecht R, Murphy J, Gerisch G. Coronin involved in phagocytosis: dynamics of particle-induced relocalization visualized by a green fluorescent protein Tag. Cell. 1995; 83:915–924. [PubMed: 8521515]
32. de Hostos EL. The coronin family of actin-associated proteins. Trends in cell biology. 1999; 9:345–350. [PubMed: 10461187]
33. Goode BL, Wong JJ, Butty AC, Peter M, McCormack AL, Yates JR, Drubin DG, Barnes G. Coronin promotes the rapid assembly and cross-linking of actin filaments and may link the actin and microtubule cytoskeletons in yeast. The Journal of cell biology. 1999; 144:83–98. [PubMed: 9885246]
34. Cai L, Marshall TW, Uetrecht AC, Schafer DA, Bear JE. Coronin 1B coordinates Arp2/3 complex and cofilin activities at the leading edge. Cell. 2007; 128:915–929. [PubMed: 17350576]
35. Gandhi M, Achard V, Blanchoin L, Goode BL. Coronin switches roles in actin disassembly depending on the nucleotide state of actin. Molecular cell. 2009; 34:364–374. [PubMed: 19450534]
36. Ge P, Durer ZA, Kudryashov D, Zhou ZH, Reisler E. Cryo-EM reveals different coronin binding modes for ADP- and ADP-BeFx actin filaments. Nature structural & molecular biology. 2014; 21:1075–1081.
37. Muhlrad A, Kudryashov D, Michael Peyser Y, Bobkov AA, Almo SC, Reisler E. Cofilin induced conformational changes in F-actin expose subdomain 2 to proteolysis. Journal of molecular biology. 2004; 342:1559–1567. [PubMed: 15364581]
38. Oztug Durer ZA, Diraviyam K, Sept D, Kudryashov DS, Reisler E. F-actin structure destabilization and DNase I binding loop: fluctuations mutational cross-linking and electron microscopy analysis of loop states and effects on F-actin. Journal of molecular biology. 2010; 395:544–557. [PubMed: 19900461]
39. Faulstich H, Schafer AJ, Weckauf M. The dissociation of the phalloidin-actin complex. Hoppe-Seyler's Zeitschrift fur physiologische Chemie. 1977; 358:181–184.
40. Balcer HI, Goodman AL, Rodal AA, Smith E, Kugler J, Heuser JE, Goode BL. Coordinated regulation of actin filament turnover by a high-molecular-weight Srv2/CAP complex, cofilin, profilin, and Aip1. Curr Biol. 2003; 13:2159–2169. [PubMed: 14680631]

41. Bryan KE, Rubenstein PA. An intermediate form of ADP-F-actin. The Journal of biological chemistry. 2005; 280:1696–1703. [PubMed: 15536092]
42. Blanchoin L, Pollard TD. Mechanism of interaction of Acanthamoeba actophorin (ADF/Cofilin) with actin filaments. The Journal of biological chemistry. 1999; 274:15538–15546. [PubMed: 10336448]
43. Kueh HY, Charras GT, Mitchison TJ, Brieher WM. Actin disassembly by cofilin, coronin, and Aip1 occurs in bursts and is inhibited by barbed-end cappers. The Journal of cell biology. 2008; 182:341–353. [PubMed: 18663144]
44. Shvetsov A, Stamm JD, Phillips M, Warshaviak D, Altenbach C, Rubenstein PA, Hideg K, Hubbell WL, Reisler E. Conformational dynamics of loop 262–274 in G- and F-actin. Biochemistry. 2006; 45:6541–6549. [PubMed: 16700564]
45. Elam WA, Kang H, De La Cruz EM. Competitive displacement of cofilin can promote actin filament severing. Biochemical and biophysical research communications. 2013; 438:728–731. [PubMed: 23911787]
46. Spudich JA, Watt S. The regulation of rabbit skeletal muscle contraction. I. Biochemical studies of the interaction of the tropomyosin-troponin complex with actin and the proteolytic fragments of myosin. The Journal of biological chemistry. 1971; 246:4866–4871. [PubMed: 4254541]
47. Grintsevich EE, Phillips M, Pavlov D, Phan M, Reisler E, Muhlrad A. Antiparallel dimer and actin assembly. Biochemistry. 2010; 49:3919–3927. [PubMed: 20361759]
48. Kuhn JR, Pollard TD. Real-time measurements of actin filament polymerization by total internal reflection fluorescence microscopy. Biophysical journal. 2005; 88:1387–1402. [PubMed: 15556992]
49. Durer ZA, McGillivary RM, Kang H, Elam WA, Vizcarra CL, Hanein D, De la Cruz EM, Reisler E, Quinlan ME. Metavinculin tunes the flexibility and the architecture of vinculin-induced bundles of actin filaments. Journal of molecular biology. 2015

RESEARCH HIGHLIGHTS

- Yeast coronin accelerates binding of cofilin to actin filament sides
- Yeast coronin enhances cofilin-mediated actin filament severing
- Yeast coronin alters lateral and longitudinal contacts in F-actin
- Yeast coronin and cofilin induce distinct conformational effects on F-actin

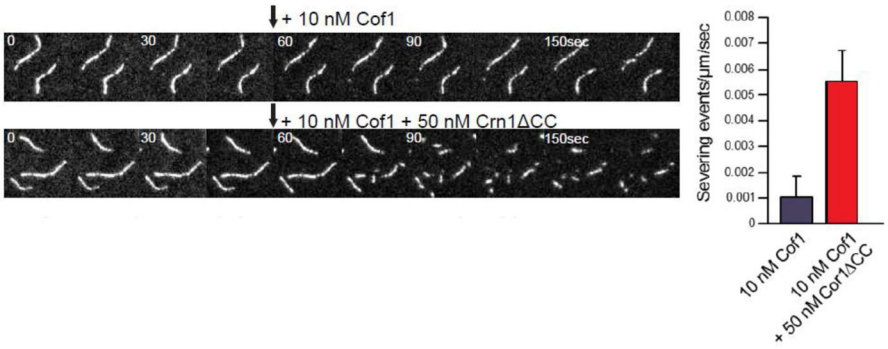

Figure 1.

Crn1ΔCC enhances Cof1-mediated severing of actin filaments. **(A)** Time points from TIRF imaging (Movie S1) showing polymerizing OG-labeled actin filaments, then (arrow) flow in of 10 nM Cof1 +/− 50 nM Crn1ΔCC. Severing events are indicated by yellow arrowheads. **(B)** Quantification of severing rates. Data are averaged from separate experiments. Error bars = SD.

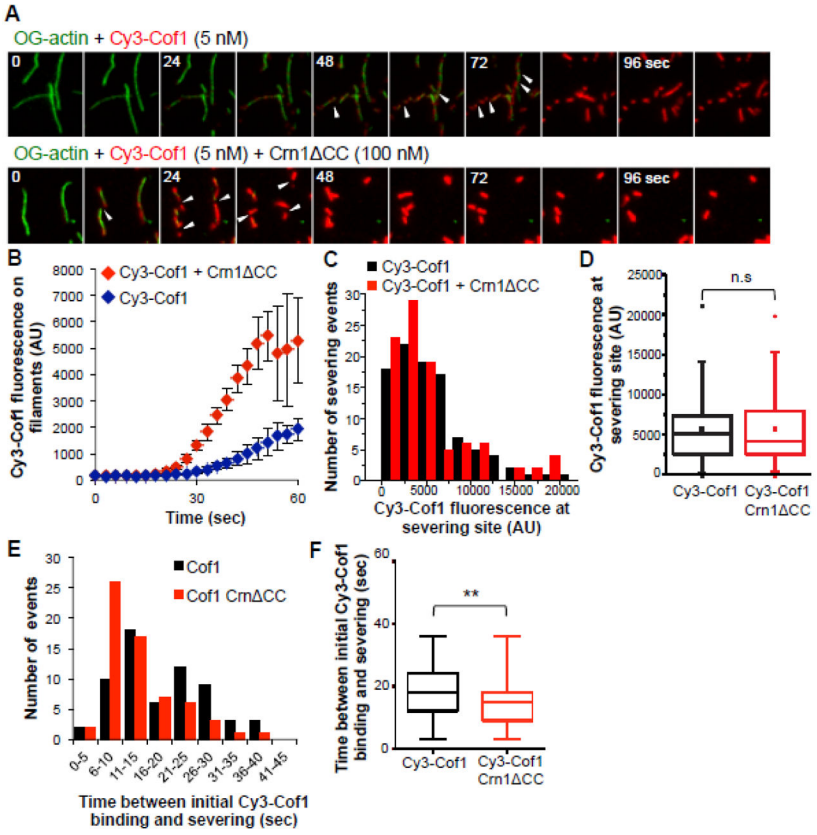

Figure 2.

Crn1ΔCC accelerates recruitment of Cy3-Cof1 to the sides of actin filaments. **(A)** Two-color TIRF microscopy of 5 nM Cy3-Cof1 interacting with preformed, tethered OG-labeled actin filaments in the presence and absence of Crn1ΔCC (100 nM). **(B)** Kinetics of Cy3-Cof1 fluorescence accumulation on actin filaments in the presence and the absence of Crn1ΔCC. Each line is an average of 10 filaments. Error bars = SD. **(C)** Distribution of Cy3-Cof1 fluorescence spot intensities on a filament just prior to a severing event, determined from experiments as in (A). **(D)** Box plots showing the 25th percentile, median and 75th percentile of the distribution in (C). Error bars indicate the 10th and 90th percentiles. **(E)** Distribution of time intervals between initial appearance of Cy3-Cof1 fluorescence and a severing event, determined from experiments as in (A). **(F)** Box plots showing the 25th percentile, median and 75th percentile of the distribution in (E). Error bars indicate the 10th and 90th percentiles. Statistical significance in (D) and (F) was determined using an unpaired T-test ($p < 0.05$).

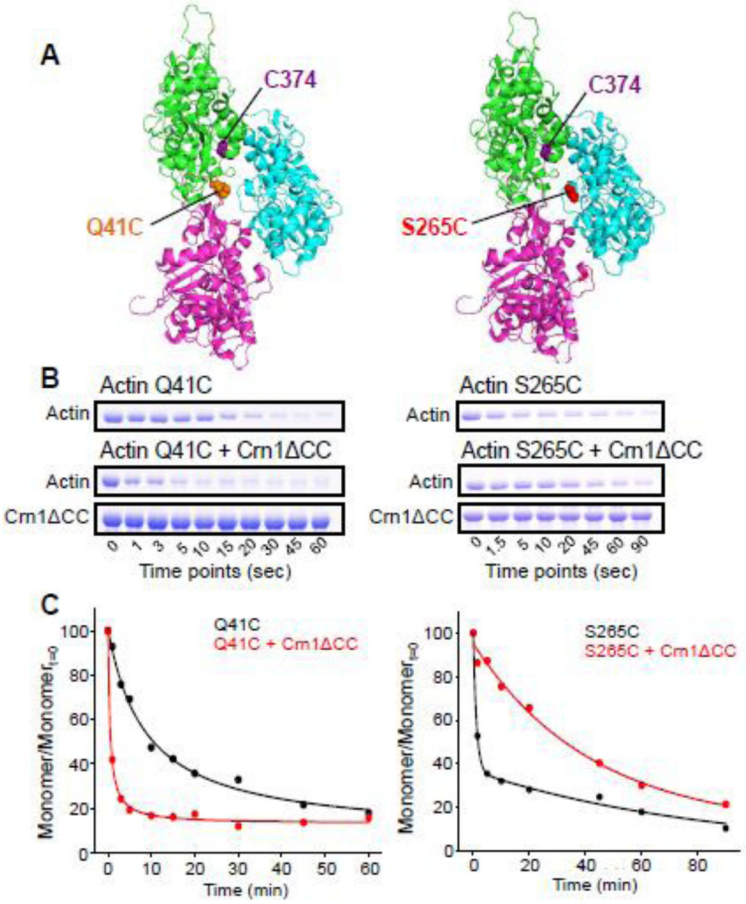

Figure 3.

Crn1ΔCC alters lateral and longitudinal contacts in F-actin. **(A)** Cartoons of F-actin showing mutated residues Q41C (left) or S265C (right), and the endogenous C374. **(B)** Cross-linking of Q41C mutant yeast actin (left) or S265C mutant yeast actin (right) was induced by $CuSO_4$ and stopped at the indicated time points. Progress of cross-linking was monitored by disappearance of the actin monomer band on non-reducing SDS-PAGE. **(C)** Densitometric quantification of actin monomer band decay based on experiments as shown in (B), in the presence and absence of Crn1ΔCC. Data were averaged from three independent experiments.

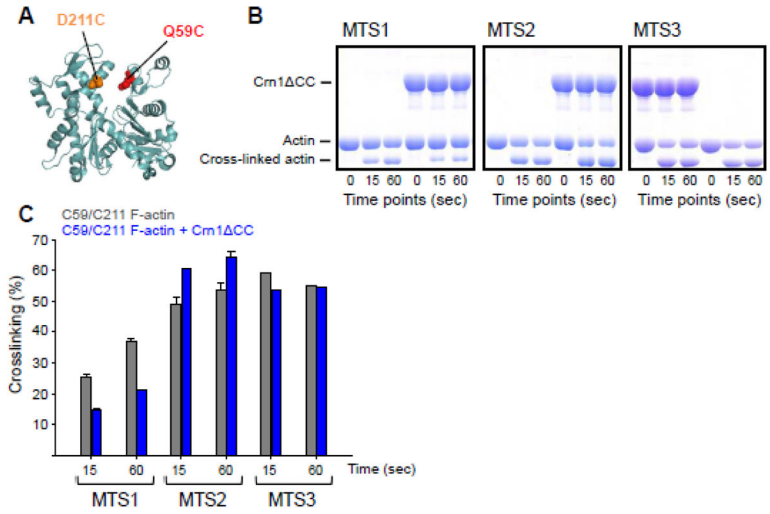

Figure 4.

CrnΔ1CC reduces the flexibility of the nucleotide-binding cleft. **(A)** Cartoon of G-actin showing mutated residues Q59C and D211C. **(B)** Cross-linking of 10 μM mutant actin ± 10 μM Crn1ΔCC was induced in the presence of MTS1 (5.4Å), MTS2 (5.9Å) or MTS3 (6.4Å) and analyzed by non-denaturing SDS-PAGE. **(C)** Cross-linking percentage of Q59C/D211C F-actin in the absence (grey bars) and presence (blue bars) of Crn1ΔCC. Relative intensities of protein bands were determined by densitometry. Cross-linking efficiency (%) was estimated from the gel bands as follows: [total actin (before the reaction) − uncross-linked actin monomer left after cross-linking time]/total actin (n=3).

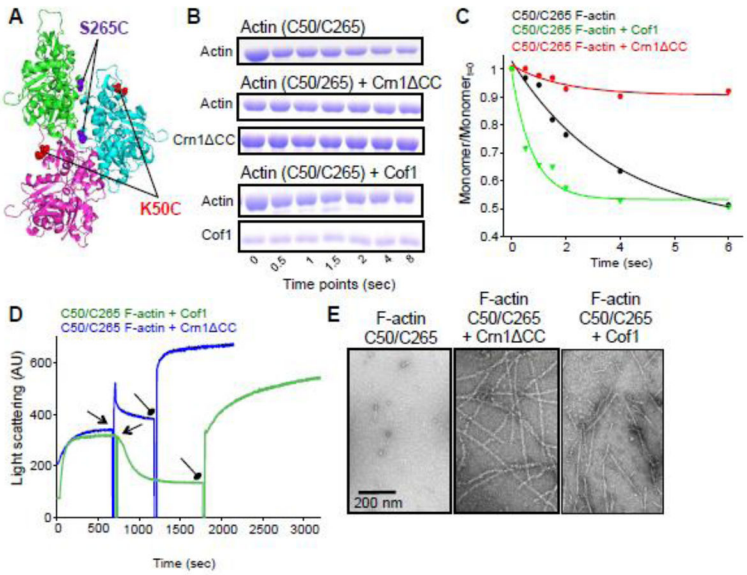

Figure 5.

Crn1ΔCC and Cof1 have opposite conformational effects on F-actin. (A) Cartoon of F-actin model showing mutated residues K50C and S265C. (B) Cross-linking of C50/C265 was induced by $CuSO_4$ and stopped at the indicated time points. Progress of cross-linking was followed by disappearance of the actin monomer band on non-reducing SDS-PAGE. (C) Densitometric quantification of actin monomer band decay, based on experiments as shown in (B). Data were averaged from three independent experiments. (D) Polymerization of 10 μM C50/C265-actin was started by the addition of 20 μM $CuSO_4$ (arrow). At the time points indicated by (● arrows), 10 μM Crn1ΔCC (blue trace) or 10 μM Cof1 (green trace) was added and polymerization was followed as the increase in light scattering. A.U., arbitrary units. (E) EM image showing the products of polymerization of C50/C265 F-actin alone, with Crn1ΔCC or with Cof1.

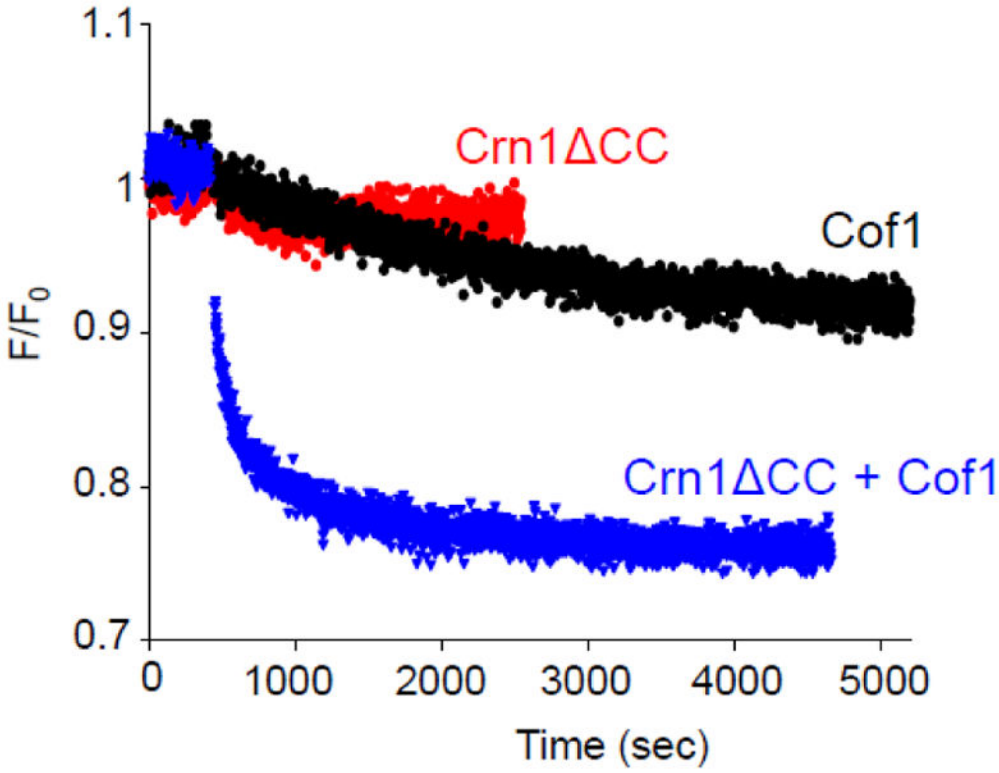

Figure 6.

Crn1ΔCC and Cof1 synergistically increase the release of rhodamine phalloidin from F-actin. Yeast F-actin (5.0 μM) was stabilized with a rhodamine phalloidin/phalloidin mixture and after recording the initial rhodamine phalloidin fluorescence, the release of rhodamine phalloidin was monitored by following the decrease in fluorescence intensity (λ_{em}=575 nm) upon the addition of Cof1 (5.5 μM, black curve), Crn1ΔCC (5.5 μM, red curve), or both (5.5 μM both, blue curve).